

HOSTED BY



ELSEVIER

Genomics Proteomics Bioinformatics

www.elsevier.com/locate/gpb
www.sciencedirect.com



ORIGINAL RESEARCH

In vitro Transcriptome Analysis of Two Chinese Isolates of *Streptococcus suis* Serotype 2



Dake Zhang^{1,#}, Nan Du^{1,#}, Sufang Ma^{2,#}, Qingtao Hu^{1,3}, Guangwen Lu², Wei Chen¹, Changqing Zeng^{1,*}

¹ CAS Key Laboratory of Genomic and Precision Medicine, Beijing Institute of Genomics, Chinese Academy of Sciences, Beijing 100101, China

² CAS Key Laboratory of Pathogenic Microbiology and Immunology, Institute of Microbiology, Chinese Academy of Sciences, Beijing 100101, China

³ University of Chinese Academy of Sciences, Beijing 100190, China

Received 30 October 2014; revised 9 November 2014; accepted 13 November 2014
Available online 16 December 2014

Handled by Wuju Li

KEYWORDS

Streptococcus suis serotype 2;
Transcriptome;
Novel transcripts;
sRNA;
Virulence factor

Abstract The *Streptococcus suis* serotype 2 (*S. suis* 2) isolates 05ZYH33 and 98HAH33 have caused severe human infections in China. Using a strand-specific RNA-seq analysis, we compared the *in vitro* transcriptomes of these two Chinese isolates with that of a reference strain (P1/7). In the 89K genomic island that is specific to these Chinese isolates, a toxin–antitoxin system showed relatively high levels of transcription among the *S. suis*. The known virulence factors with high transcriptional activity in these two highly-pathogenic strains are mainly involved in adhesion, biofilm formation, hemolysis and the synthesis and transport of the outer membrane protein. Furthermore, our analysis of novel transcripts identified over 50 protein-coding genes with one of them encoding a toxin protein. We also predicted over 30 small RNAs (sRNAs) in each strain, and most of them are involved in riboswitches. We found that six sRNA candidates that are related to bacterial virulence, including *cspA* and *rli38*, are specific to Chinese isolates. These results provide insight into the factors responsible for the difference in virulence among the different *S. suis* 2 isolates.

Introduction

The *Streptococcus suis* serotype 2 (*S. suis* 2) are Gram-positive bacteria and represent the leading cause of porcine diseases [1].

They can also infect humans that have direct contact with infected swine, causing meningitis, hearing loss and septic shock [1–3]. In China, two large-scale outbreaks of severe human infections of *S. suis* 2 were reported in 1998 and 2005, respectively [4]. *S. suis* 2 is also one of the major pathogens associated with bacterial meningitis in other Asian areas, such as Hong Kong and Thailand [5–7]. Therefore, it poses a significant threat to public health [8].

The known markers of *S. suis* 2 include capsular polysaccharide (CPS), muramidase release protein (MRP), elongation

* Corresponding author.

E-mail: czeng@big.ac.cn (Zeng C).

Equal contribution.

Peer review under responsibility of Beijing Institute of Genomics, Chinese Academy of Sciences and Genetics Society of China.

<http://dx.doi.org/10.1016/j.gpb.2014.11.001>

1672-0229 © 2014 The Authors. Production and hosting by Elsevier B.V. on behalf of Beijing Institute of Genomics, Chinese Academy of Sciences and Genetics Society of China.

This is an open access article under the CC BY-NC-ND license (<http://creativecommons.org/licenses/by-nc-nd/3.0/>).

factor (EF) and sulysin (SLY) [9]. The capsule is one of the key factors involved in bacterial pathogenicity. For instance, *S. suis* capsular polysaccharide inhibits phagocytosis through destabilization of lipid microdomains and prevents lactosylceramide-dependent recognition [9]. The capsule also protects the bacteria against phagocytosis. The Ssa protein of *S. suis* 2, a surface-anchored fibronectin-binding protein, also facilitates epithelial cell invasion [7]. In bacteria, two-component systems (TCSs) are crucial devices that enable their adaption to changing growth conditions, and hence affect bacterial virulence. More than 15 TCSs have been reported in *S. suis* 2 so far [4]. They are believed to facilitate bacterial adherence to mucosal epithelium cells, to participate in the process of capsular wall formation, and they have been shown to help bacteria survive and proliferate in *in vivo* mouse models [10–15]. Moreover, other regions of the *S. suis* 2 genome may contribute to its virulence as well [16].

In 2007, Chen et al. sequenced the whole genomes of the Chinese isolates of two *S. suis* 2 strains 05ZYH33 and 98HAH33, which were involved in the two aforementioned outbreaks, respectively [4]. Comparison of the genomes of these two Chinese strains with that of the reference genome, P1/7, suggested that an 89K genomic island (GI) is responsible for the altered pathogenicity of the Chinese isolates. Further analyses revealed that this 89K GI contains important virulence factors, including zeta toxin, TCS and ATP-binding cassette (ABC) transporters. Functional experiments revealed a dramatic decrease in the virulence of 05ZYH33 following the disruption of the TCS in the 89K GI [15]. Moreover, this 89K GI can be transmitted across different strains, and thus might represent a mechanism that enables *S. suis* 2 to adapt quickly to the local environment [17].

Although gene prediction methods have been widely applied in bacterial genome annotation, the use of next-generation sequencing (NGS) technology often reveals various novel transcripts, especially those belonging to the diverse small RNA (sRNA) families [18]. The regulatory role of these sRNAs in gene expression and in bacterial virulence is only now being slowly elucidated [19–22]. Here, we provide the first RNA-seq datasets from two Chinese isolates of *S. suis* 2.

Results

Transcriptome analysis pipeline and data statistics

We performed a strand-specific sequencing of the *in vitro* transcriptomes of three *S. suis* 2 strains, including the two highly-virulent isolates 05ZYH33 and 98HAH33, and the reference strain P1/7. About 27–40 million uniquely-mapped reads were

obtained for each transcriptome, while achieving a good sequencing depth for further analysis (Table 1 and Figure S1). The regions with a single-nucleotide resolution sequencing coverage greater than $3 \times$ accounted for over 93%, 92% and 95% of the whole genome of the 05ZYH33, 98HAH33 and P1/7 strains, respectively (data not shown). These percentages were similar to those previously reported for *Bacillus anthracis* (94%), *Burkholderia mallei* (95%) and *Sulfolobus solfataricus* (89.5%) [23–25], demonstrating the reliability of our datasets.

Analysis of differential gene expression in homologous genes

To compare the gene expression levels among the three isolates, we first identified their homologous genes (Materials and methods and Figure 1). Overall, 1672 homologous genes were identified in the three stains, and the differentially expressed genes (DEGs) were determined using three software packages (Materials and methods). In total, 318 genes were differentially expressed between 05ZYH33 and P1/7 strains, and 231 DEGs were identified between 98HAH33 and P1/7 strains. There were 120 DEGs common to these two comparisons (Table S1). Among them, expression of about 50% genes was upregulated

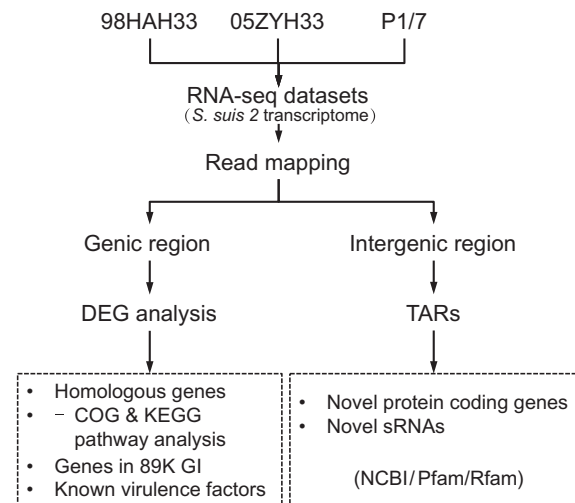


Figure 1 The pipeline for *S. suis* 2 transcriptome analysis

Sequencing reads were first mapped to reference genome. Sequencing reads in genic region are used to calculate the expression levels of each gene, and then DEGs are identified among three isolates. Sequencing reads found in intergenic regions are used to define novel TARs, which are annotated based on homology analysis. DEG, differentially-expressed gene; TAR, transcriptionally-active region; GI, genomic island.

Table 1 Transcriptome sequencing and mapping statistics for the three *S. suis* 2 strains

Strain	No. of raw reads	No. of reads after rRNA removal	No. of mapped reads	No. of uniquely-mapped reads	No. of TARs	
					+ strand	- strand
05ZYH33	50,554,946	50,553,160 (99.999%)	47,527,320 (94.01%)	39,020,066 (82.1%)	1285	1216
98HAH33	33,429,474	33,406,466 (99.93%)	31,581,564 (94.54%)	27,182,870 (86.07%)	1332	1211
P1/7	47,162,906	47,139,616 (99.95%)	44,877,096 (95.2%)	40,313,416 (92.43%)	1222	1216

Note: Different coverage thresholds were used for identification of TARs (> 70 bp in length) in the three strains, which are $9 \times$ for 05ZYH33, $7 \times$ for 98HAH33 and $16 \times$ for P1/7, respectively. All the percentages in the parenthesis beside the absolute read No. were obtained by dividing the target read number by the one listed in the preceding column on its left. For example, percentage of “No. of reads after rRNA removal” = “No. of reads after rRNA removal” (50,553,160)/“No. of raw reads” (50,554,946) = 99.99%. TAR, transcriptionally-active region.

2–4 folds in the two Chinese isolates, and these genes shared similar expression patterns in the two Chinese strains when compared with that in P1/7 (Figure 2). Interestingly, most upregulated genes encode surface-anchored proteins, whereas the downregulated genes were enriched in the β -glucoside-specific phosphotransferase system (PTS) (Table S1). The most downregulated gene in the Chinese strains was SSU05_1491/SSU98_1502 (SSU1310, the homologous gene in P1/7), which encodes a transcriptional anti-terminator (Table S1).

The two Chinese isolates shared 246 additional homologous genes (not shown). Among the 10 most highly-expressed

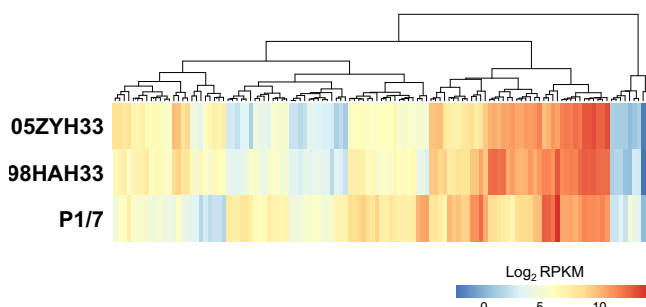


Figure 2 DEGs in the Chinese isolates shared a similar expression pattern

In total 120 DEGs are shared by both Chinese isolates when compared with P1/7. The hierarchical heatmap (R package: pheatmap) illustrates transcriptional levels (\log_2 ratios of RPKM, scale is shown at the bottom) for all the DEGs in three strains. The expression levels of DEGs in two Chinese isolates are more similar compared to P1/7.

genes comparing with the reference isolate, eight were seen in both isolates. For example, SSU05_0582/SSU98_0586 encodes the IS5 family transposase, whereas SSU05_0179/SSU98_0181 are exoprotein A genes from the RTX family and the encoded protein was reported to cause hemolysis [26].

Clusters of orthologous group analysis

For all the genes annotated in previous studies, further scrutiny of the gene expression data revealed that 2092, 2094 and 1890 genes were identified with reads per kilo bases per million reads (RPKM) > 1, which accounted for 92.8%, 92.9% and 94% of all genes in 05ZYH33, 98HAH33 and P1/7 strains, respectively. Among them, 1737, 1712 and 1559 genes were annotated with known clusters of orthologous groups (COG) functions in 05ZYH33, 98HAH33 and P1/7, respectively. A similar gene distribution in COGs was observed for all three strains (Figure S2), which indicates the similar biological processes can be observed in all three isolates.

To investigate the biological processes and show different activity in two Chinese isolates comparing with P1/7 isolate, we further analyzed the classification of the 120 aforementioned DEGs and found that 96 genes were classified into four major functional categories with 16 subgroups (Figure 3). Among the homologous genes that were upregulated in the Chinese isolates, 15 were significantly enriched in the functional group of translation, ribosomal structure and biogenesis ($P < 0.000005$, Fisher's exact test). Meanwhile, among the homologous genes that were downregulated in the Chinese isolates, 22 significantly-enriched genes ($P < 0.0000005$, Fisher's exact test) fall into the COG subgroup of carbohydrate transport and metabolism.

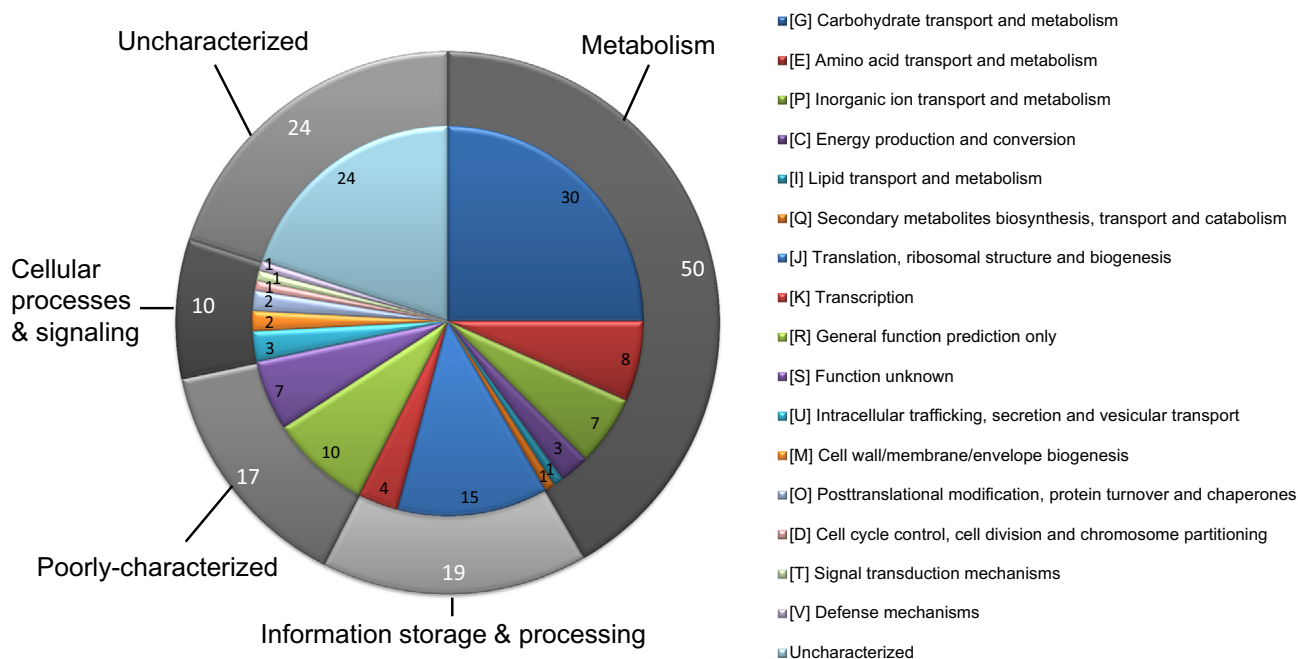


Figure 3 COG analysis of homologous DEGs

The pie chart showed the COG analysis for the classification of homologous DEGs in the 05ZYH33 and 98HAH33 isolates, compared to the P1/7 reference strain. The general categories are indicated on the outer circle and the subgroups are indicated in the inner circle with the number of genes belonging to each group listed.

KEGG pathway analysis

KEGG pathway mapping revealed that the biological processes that were abundant in the DEGs mainly include PTS, glycolysis/gluconeogenesis and ribosome (Table 2 and Figures S3–S5) ($P < 0.01$).

Although all three strains shared the species-specific components in the PTS pathway, fewer transcripts of the Man family genes were detected in 98HAH33 and 05ZYH33 (Figure S3). Conversely, most Gk family genes except *BglF* (PTS system, β -glucosides-specific II component) had more transcripts detected in the two Chinese isolates. However, it is of note that *BglF* is the most downregulated gene in PTS pathway, suggesting a reduced conversion from β -glucosides to phospho- β -glucosides.

In addition, the transcriptional level of the genes (SSU05_0398/SSU98_0384) responsible for transforming arbutin and salicin into arbutin-6p and salicin-6p, respectively, was increased, whereas the transcriptional activity of downstream 6-phospho- β -glucosidase (Enzyme Commission number: 3.2.1.86, encoded by SSU05_1489/SSU98_1500 and

SSU05_2079/SSU98_2083) was extensively repressed in the two Chinese isolates (Figure S4). Therefore, their products arbutin-6p and salicin-6p may accumulate in the bacterial metabolites of the two Chinese isolates.

Differential expression levels of known virulence factors

It is believed that two Chinese isolates are more pathogenic than P1/7 isolate, and we next analyzed transcriptional level of all known virulence factors in three isolates. Our analysis indicated that these three isolates had 96 known virulence factors in common according to VFDB. However, only the gene encoding ORF46-putative ABC transporter membrane protein (SSU05_0111/SSU98_0114/SSU0114, VFG1497) was highly expressed in the Chinese isolates; whereas expression of three genes including SSU05_0148/SSU98_0152/SSU0147, SSU05_1381/SSU98_1396/SSU0466 and SSU05_1387/SSU98_1401/SSU1215, were downregulated (Table 3). We then analyzed all the DEGs encoding virulence factors shared by P1/7 and either 05ZYH33 or 98HAH33 rather than both of

Table 2 DEGs in PTS and glycolysis/gluconeogenesis pathways

Strain	Gene symbol	Gene ID	FC	Protein
<i>PTS pathway</i>				
98HAH33	<i>LacF</i>	SSU98_1051	3.05	PTS cellobiose-specific component IIA
	<i>Pts/Crr</i>	SSU98_0384	1.92	PTS IIC component, glucose
	<i>AgaW</i>	SSU98_1233	-1.37	PTS, mannose
	<i>UlaA</i>	SSU98_0191	-1.38	Hypothetical protein
	<i>ManY</i>	SSU98_0439	-1.43	PTS, mannose
	<i>LacE</i>	SSU98_0210	-1.49	PTS cellobiose-specific component IIC
	<i>CelB</i>	SSU98_2074	-1.62	PTS cellobiose-specific component IIC
	<i>CelB</i>	SSU98_0712	-1.66	PTS cellobiose-specific component IIC
	<i>AgaE</i>	SSU98_1232	-1.71	PTS, mannose
	<i>ManZ</i>	SSU98_0440	-1.80	PTS, mannose
	<i>BglF</i>	SSU98_1501	-6.74	PTS IIC component, glucose
05ZYH33	<i>LacF</i>	SSU05_1038	1.11	PTS cellobiose-specific component IIA
	<i>Pts/Crr</i>	SSU05_0398	1.56	PTS IIC component, glucose/maltose/ <i>N</i> -acetylglucosamine-specific
	<i>AgaW</i>	SSU05_1218	-2.59	PTS, mannose/fructose/ <i>N</i> -acetylgalactosamine-specific component IIC
	<i>UlaA</i>	SSU05_0189	-1.77	PTS system ascorbate-specific transporter subunit IIC
	<i>ManY</i>	SSU05_0451	-2.19	PTS, mannose/fructose/ <i>N</i> -acetylgalactosamine-specific component IIC
	<i>LacE</i>	SSU05_0212	-3.43	PTS cellobiose-specific component IIC
	<i>CelB</i>	SSU05_2071	-1.67	PTS cellobiose-specific component IIC
	<i>CelB</i>	SSU05_0713	-3.26	PTS cellobiose-specific component IIC
	<i>AgaE</i>	SSU05_1217	-3.05	PTS, mannose/fructose/ <i>N</i> -acetylgalactosamine-specific component IID
	<i>ManZ</i>	SSU05_0452	-2.33	PTS, mannose/fructose/ <i>N</i> -acetylgalactosamine-specific component IID
	<i>BglF</i>	SSU05_1490	-5.40	PTS IIC component, glucose/maltose/ <i>N</i> -acetylglucosamine-specific
Strain	EC ID	Gene ID	FC	Protein
<i>Glycolysis/gluconeogenesis pathway</i>				
98HAH33	2.7.1.69	SSU98_0384	1.92	PTS IIC component, glucose
	3.2.1.86	SSU98_2083	-1.02	Alpha-galactosidase
	1.1.1.1	SSU98_0274	-1.63	AdhA
	1.1.1.1	SSU98_0275	-1.92	Bifunctional acetaldehyde-CoA
	3.2.1.86	SSU98_1500	-6.14	Beta-glucosidase
05ZYH33	2.7.1.69	SSU05_0398	1.56	PTS IIC component, glucose/maltose/ <i>N</i> -acetylglucosamine-specific
	3.2.1.86	SSU05_2079	-1.69	Alpha-galactosidase/6-phospho-beta-glucosidase
	1.1.1.1	SSU05_0279	-2.29	Alcohol dehydrogenase
	1.1.1.1	SSU05_0280	-3.01	Bifunctional acetaldehyde-CoA/alcohol dehydrogenase
	3.2.1.86	SSU05_1489	-5.05	Beta-glucosidase/6-phospho-beta-glucosidase/beta-galactosidase

Note: FC stands for fold change, which was calculated by \log_2 expression of the respective Chinese isolate/expression of P1/7. PTS, phospho-transferase system. EC ID refers to the enzyme commission number in KEGG.

Table 3 Differentially-expressed virulence factors

Category	VFDB ID	Gene ID	RPKM	Gene symbol	Protein
<i>All three isolates</i>					
Upregulated	VFG1497	SSU05_0111/SSU98_0114/SSU0114	152.6/292.4/79.3	<i>ORF46</i>	Putative ABC transporter membrane protein
Downregulated	VFG1855	SSU05_0148/SSU98_0152/SSU0147	2680.4/2435.8/3243.0	<i>htpB</i>	Hsp60, 60 K heat shock protein HtpB
	VFG0869	SSU05_1381/SSU98_1396/SSU0466	147.1/212.3/679.6	<i>aatC</i>	AatC ATB binding protein of ABC transporter
	VFG0594	SSU05_1387/SSU98_1401/SSU1215	135.3/359.7/912.5	<i>pipD</i>	Pathogenicity island encoded protein: SPI3
<i>05ZYH33/98HAH33-specific</i>					
	VFG0317	SSU05_1281/SSU98_1295	119.3/90.4	<i>rfaI</i>	Lipopolysaccharide 1,2-glucosyltransferase
	VFG2194	SSU05_2090/SSU98_2093	64.5/81.1	<i>fsrA</i>	Unknown
	VFG1462	SSU05_0588/SSU98_0592	23.4/33.5	10015	Putative IS protein
	VFG1513	SSU05_0587/SSU98_0591	15.2/16.1	<i>s0025</i>	IS66-like transposase
	VFG0284	SSU05_0973/SSU98_0987	0.8/1.9	<i>cag5 (virD4)</i>	Cag pathogenicity island protein, DNA transfer protein
	VFG2173	SSU05_0965/SSU98_0978	0.6/1.0	<i>asal</i>	Aggregation substance Asa1
	VFG1453	SSU05_0979/SSU98_0993	0.2/0.7	<i>ORF2</i>	Putative DNA methylase
<i>Well-known factors</i>					
Upregulated	–	SSU05_0753/SSU98_0756/SSU0706	4575.6/6524.3/2045.4	<i>mrp</i>	Muramidase release protein
	–	SSU05_0155/SSU98_0158/SSU0153	19380.7/20694.6/16530.14	<i>gapdh</i>	Glyceraldehyde-3-phosphate dehydrogenase
Downregulated	–	SSU05_0841/SSU98_0841/SSU0785	423.3/339.3/506.326	<i>lepA</i>	Elongation factor
Mixed	–	SSU05_1403/SSU98_1416/SSU1231	137.9/677.642/440.004	<i>sly</i>	Suilysin
	–	SSU05_0564/SSU98_0567/SSU0515	1026.3/441.9/704.4	<i>cps2A</i>	Capsular polysaccharide

Note: ID for the genes, which essentially encode the same virulence factor in the strains and their corresponding RPKM, were listed in the order of 05ZYH33, 98HAH33 and P1/7. For example, Gene ID SSU05_0111/SSU98_0114/SSU0114 represent SSU05_0111 in 05ZYH33, SSU98_0114 in 98HAH33 and SSU0114 in P1/7, which all encode *ORF46*, and their expression level in terms of RPKM is 152.6 in 05ZYH33, 292.4 in 98HAH33 and 79.3 in P1/7, respectively. Mixed means that the expression of genes was upregulated in one Chinese isolate but downregulated in the other isolate.

them. The KEGG analysis revealed that the ABC transporter pathway was enriched in the highly-expressed virulence factors in the 98HAH33 and 05ZYH33 (Table S2).

Furthermore, seven other virulence factors were found to be specific to the two virulence strains (Table 3). For instance, The RPKM value of SSU05_1281/SSU98_1295 ranked the top among those of the seven factors. SSU05_1281/SSU98_1295 encodes lipopolysaccharide 1,2-glucosyltransferase (RfaJ), which adds a glucose (II) group on the galactose (I) group of lipopolysaccharides (LPS). The gene expression of well-known factors such as *eps*, *mvp*, *lepA* (EF4) and *sly* are also listed in Table 3.

Transcriptional activity of the 89K GI in 98HAH33 and 05ZYH33

89K GI is specific to two pathogenic Chinese isolates. In this region, 98HAH33 and 05ZYH33 strains have 78 homologous

genes. Among them, 59 genes had ≥ 3 sequencing reads recovered in the RNA-seq datasets. The distribution of the RPKM values for all of these genes in the two strains showed that highest number of genes had RPKM values < 1 , indicating a low transcriptional activity during *in vitro* culture (Figure 4). Three known virulence factors specific to the Chinese isolates, including VFG0284, VFG2173 and VFG1453 (Table 3), were located in this GI as well.

Six genes with high transcriptional activity were seen in both strains (Table 4). According to the STRING database (Search Tool for the Retrieval of Interacting Genes/Proteins, <http://www.string-db.org/>), a signal recognition particle GTPase encoded by SSU05_0936/SSU98_0943 and a transcriptional regulator encoded by SSU05_0937/SSU98_0944 can form a toxin-antitoxin (TA) system. This TA system showed a high homology with the PezAT chromosomal TA system of the human pathogen *Streptococcus pneumoniae* [27].

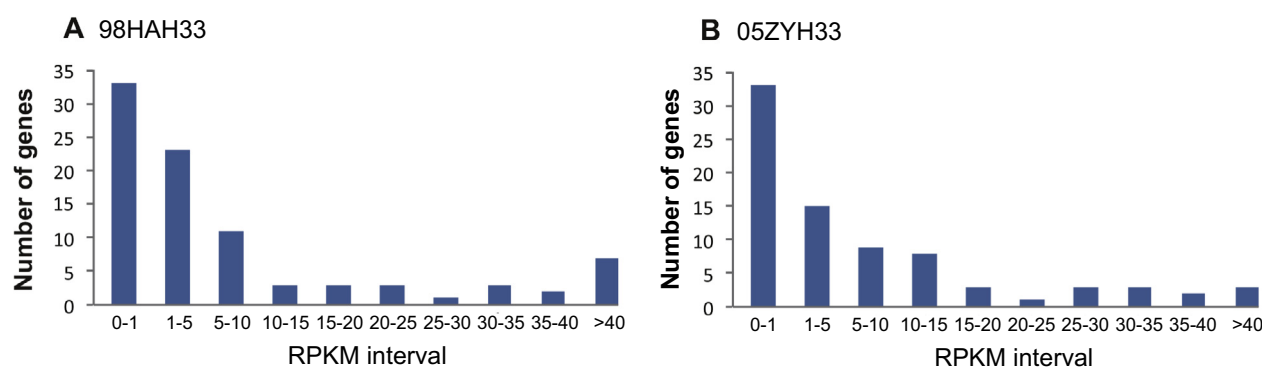


Figure 4 Transcriptional activity of genes located in 89K GI of the Chinese isolates

The histogram demonstrates the distribution of genes at different transcription level (RPKM values) for 98HAH33 (A) and 05ZYH33 (B). The group “RPKM < 1 ” contains the highest number of genes, indicating the low transcriptional activity of 89K GI region during *in vitro* incubation of these isolates.

Table 4 Top 10 most highly-expressed genes specific to the Chinese isolates

Strain	Rank	Gene ID	RPKM	COG ID	Protein
05ZYH33	1	SSU05_0582	2067.935	COG3039L	IS5 family transposase
	2	SSU05_1895	1461.981	–	Hypothetical protein
	3	SSU05_1896	1428.723	COG3871R	Hypothetical protein
	4	SSU05_0177	1284.939	–	Extracellular protein
	5	SSU05_0178	1190.736	–	Epf-like protein
	6	SSU05_0179	1149.505	–	RTX family exoprotein A gene
	7	SSU05_0373	1073.18	COG1335Q	Nicotinamidase-like amidase
	8	SSU05_0372	782.191	COG1670J	Histone acetyltransferase HPA2-like acetyltransferase
	9	SSU05_0553	664.709	–	Hypothetical protein
	10	SSU05_1990	660.201	COG3481R	HD-superfamily hydrolase
98HAH33	1	SSU98_0181	2124.663	–	RTX family exoprotein A gene
	2	SSU98_0586	1986.35	COG3039L	IS5 family transposase
	3	SSU98_0179	1799.871	–	Extracellular protein
	4	SSU98_0180	1684.485	–	Epf-like protein
	5	SSU98_1014	1076.934	–	Hypothetical protein
	6	SSU98_0364	1049.139	COG1335Q	Nicotinamidase-like amidase
	7	SSU98_1026	986.816	COG0448G	ADP-glucose pyrophosphorylase
	8	SSU98_1897	972.083	–	Hypothetical protein
	9	SSU98_0363	876.425	COG1670J	Histone acetyltransferase HPA2-like acetyltransferase
	10	SSU98_1898	796.214	COG3871R	Hypothetical protein

Note: The toxin-antitoxin system components with high transcription level in both virulent isolates are highlighted in bold. RPKM, reads per kilo bases per million reads; COG, clusters of orthologous groups.

Novel transcripts identified in the transcriptomes of three isolates

Gene annotation of these three isolates is mainly based on prediction method, and we used transcriptome data to find novel genes in three genomes. In all, over 50 novel transcriptionally-active regions (TARs) were identified in intergenic regions of the two Chinese isolates (see Material and Method). Most of them were homologous to genes that only encode hypothetical proteins (Table S3). Only 9 and 8 TARs had homologous genes with known functions for the 05ZYH33 and 98HAH33, respectively (Table 5). In particular, one TAR predicted to encode a toxin protein was identified in both isolates.

We also predicted 56 sRNAs in three isolates. Among them, 12 sRNAs related to bacterial virulence are listed in Table 6. It is of note that *rliD* and *RatA* were detected in all three isolates.

In addition, the two Chinese isolates also had the sRNAs *cspA* and *rli38* in common and the latter was located at the 89K GI. For the rest sRNAs, over 27% (12/44) of the novel sRNAs were involved in riboswitches (Table S4).

Discussion

Known virulence factors contributing to the pathogenicity of *S. suis* 2

Although *in vitro* transcriptomes do not resemble *in vivo* ones, this analysis nonetheless illustrated the overall expression patterns for all the known virulence factors of *S. suis* 2 during *in vitro* incubation. The genes encoding the five well-known factors, *mrp*, *gapdh*, *sly*, *lepA* (EF4) and *cps2A*, all had

Table 5 Novel TARs with homologous genes having known functions

Strain	TAR ID	Strand	Start position	End position	Length	Homologous gene	Genome ID	Protein
05ZYH33	05zyh33_new1	+	24,422	24,911	490	GI: 386587281	NC_017622.1	Rod shape-determining protein MreD
	05zyh33_new6	+	84,830	84,947	118	GI: 403060703	NC_018526.1	50S ribosomal protein L36
	05zyh33_new7	+	208,869	209,049	181	GI: 403060703	NC_018526.1	Copper-transporting ATPase
	05zyh33_new8	–	464,948	465,239	292	GI: 386587281	NC_017622.1	Transposase
	05zyh33_new16	+	566,368	566,536	169	GI: 403060703	NC_018526.1	<i>N</i> -acetylneuraminate cytidyltransferase
	05zyh33_new22	–	933,091	933,265	175	GI: 386585202	NC_017621.1	Lantibiotic protein
	05zyh33_new23	–	999,593	999,674	82	GI: 403060703	NC_018526.1	Helicase subunit of the DNA excision repair complex
	05zyh33_new34	–	1,578,674	1,578,830	157	GI: 403060703	NC_018526.1	Serum opacity factor
	05zyh33_new48	–	1,915,147	1,915,405	259	GI: 403060703	NC_018526.1	Toxin–antitoxin system, toxin protein
	98HAH33	98hah33_new5	+	84,826	84,943	118	GI: 403060703	NC_018526.1
98hah33_new7		+	208,714	208,894	181	GI: 403060703	NC_018526.1	Copper-transporting ATPase
98hah33_new17		+	566,231	566,399	169	GI: 403060703	NC_018526.1	<i>N</i> -acetylneuraminate cytidyltransferase
98hah33_new24		–	932,796	932,970	175	GI: 386585202	NC_017621.1	Lantibiotic protein
98hah33_new25		–	999,285	999,366	82	GI: 403060703	NC_018526.1	Helicase subunit of the DNA excision repair complex
98hah33_new27		–	1,116,314	1,116,593	280	GI: 403060703	NC_018526.1	Membrane associated protein
98hah33_new45		–	1,892,560	1,892,725	166	GI: 403060703	NC_018526.1	50S ribosomal protein L33
98hah33_new48		–	1,914,521	1,914,779	259	GI: 403060703	NC_018526.1	Toxin–antitoxin system, toxin protein

Note: GI number is listed for each homologous gene. TAR, transcriptionally-active region.

Table 6 Novel sRNAs potentially regulating bacterial virulence

Strain	TAR ID	Strand	TAR		Mapped with homologous genes			sRNA		Description
			Start	End	Start	End	Length	Start	End	
05ZYH33	05seq336	–	389,484	392,352	389,489	389,850	362	1	428	<i>cspA</i> : <i>cspA</i> thermoregulator
	05seq972	+	1,825,119	1,830,751	1,830,583	1,830,751	169	1	169	<i>rliD</i>: Listeria sRNA rliD
	05seq1101	+	1,993,916	1,994,224	1,993,916	1,993,992	77	10	91	<i>RatA</i>: RNA anti-toxin A
	05seq710	+	961,698	961,817	961,698	961,817	120	15	134	<i>rli38</i> : Listeria sRNA <i>rli38</i>
98HAH33	98seq331	–	391,826	392,204	391,827	392,185	359	1	428	<i>cspA</i> : <i>cspA</i> thermoregulator
	98seq1086	–	2,057,227	2,057,829	2,057,231	2,057,296	66	1	71	<i>STnc370</i> : Enterobacterial sRNA <i>STnc370</i>
	98seq1021	+	1,824,549	1,830,052	1,829,956	1,830,052	97	1	97	<i>rliD</i>: Listeria sRNA rliD
	98seq1137	+	1,993,284	1,993,592	1,993,284	1,993,360	77	10	91	<i>RatA</i>: RNA anti-toxin A
	98seq696	+	961,400	961,519	961,400	961,519	120	15	134	<i>rli38</i> : Listeria sRNA <i>rli38</i>
P1/7	17seq501	–	635,186	635,918	635,187	635,263	77	1	77	<i>isrK</i> : <i>isrK</i> Hfq binding RNA
	17seq1095	–	1,905,111	1,905,186	1,905,111	1,905,186	76	1	91	<i>RatA</i>: RNA anti-toxin A
	17seq916	+	1,736,325	1,741,929	1,741,790	1,741,929	140	1	140	<i>rliD</i>: Listeria sRNA rliD

Note: TAR, transcriptionally-active region. Mapped starts and ends indicate the region of TARs that is aligned with homologous genes. Starts and ends of sRNA indicate the corresponding part of sRNA. TARs that are shared in all three strains are highlighted in bold in description.

relatively high transcription levels comparing to other virulence factors (Table 3). In particular, although it was previously reported that inactivation of *mrp* is related to an increase in bacterial virulence [28], the two pathogenic strains had even higher transcription levels of *mrp*.

Glucose metabolism in bacteria not only reflects their priority for certain carbon sources, but also affects their virulence [29]. PTS functions as a sugar phosphorylating system and regulates diverse metabolic processes that affect the expression of many genes, especially those related to bacterial virulence [30]. In *Listeria monocytogenes*, the depletion of the *mpt* operon, which encodes the EII(t)(Man) PTS permease, resulted in increased expression of five genes in the *prfA* virulence gene cluster [31]. In this study, we observed the downregulation of four genes of the Man family in the PTS pathway, suggesting the involvement of the PTS pathway in changing the virulence of both Chinese isolates.

Downregulation of transcriptional anti-terminators may influence the virulence of the Chinese isolates

In the PTS pathway, the most significantly downregulated gene was SSU05_1490/SSU98_1501 (*BgIF*). In a recent study performed in *Escherichia coli*, *BgIF* has been shown to negatively regulate transcriptional anti-terminator proteins of the BgIG family [32]. Both Chinese isolates just have one gene that belongs to the BgIG family, SSU05_1491/SSU98_1502, with fewer transcripts identified compared to P1/7, rather than increased as predicted. Therefore, there may be other novel proteins in the BgIG family or distinctive regulatory mechanisms in *S. suis* 2, which have yet to be discovered. Nevertheless, previous studies showed that decreased activity of the transcriptional anti-terminator proteins might change the bacterial virulence [33]. For instance, the reduction in the expression of the transcriptional anti-terminator RfaH may increase the *Ag43* expression level, and thereby stimulate biofilm formation [33]. The repressed transcription of SSU05_1491/SSU98_1502 indicates that some mechanism is responsible for the change in virulence in the two Chinese isolates.

Conclusion

Here, we provided the first publicly-available RNA-seq data for three *S. suis* 2 isolates, and we highlighted the biological processes in the two highly pathogenic isolates, providing clues for mechanistic research. Furthermore, our detailed lists of novel protein-coding genes and sRNAs provide candidates for further functional investigations, especially in the regulation of bacterial virulence.

Materials and methods

Bacterial culture

The three *S. suis* 2 strains 98HAH33, 05ZYH33 and P1/7 were obtained from Institute of Microbiology, Chinese Academy of Sciences. Bacteria were grown in Todd-Hewitt Broth (THB) (Difco Laboratories, Detroit, MI, USA) supplemented with 2% yeast extract (THY) at 37 °C. The growth rates and

bacterial concentrations for all strains were determined by measuring the optical density (OD) at 600 nm each 60 min (Figure S6). All isolates reached the log/exponential phase after incubation for 5 h.

Transcriptome sequencing

Total RNA was isolated from bacteria at log/exponential phase using the SV Total RNA Isolation system (Promega), according to the manufacturer's instructions. Ribosomal RNAs were removed using the Ribo-Zero™ rRNA Removal Kit for Gram-Positive Bacteria (EPICENTRE Biotechnologies, Madison, WI). Strand-specific libraries were constructed and sequenced on the Illumina GAII platform by the Genomics and Bioinformatics Platform at the Beijing Institute of Genomics, Chinese Academy of Sciences. The raw sequencing datasets were uploaded to the NCBI SRA database (accession No: SRP043973).

Read mapping

The sequencing read quality was evaluated using the FastQC tool (<http://www.bioinformatics.babraham.ac.uk/projects/fastqc/>), and data saturation analyses were carried out using the RSeQC software [34]. Qualified reads (quality score > 20) were first filtered for ribosomal RNAs using the BWA software (<http://bio-bwa.sourceforge.net/>), and the rest were subsequently mapped to reference genomes of 98HAH33, 05ZYH33 and P1/7. The uniquely-mapped reads (MAPQ > 20) were used for further analysis. In addition, the sequencing coverage for single nucleotide of the genome as calculated using the genomeCoverageBed in BEDTools [35].

Gene expression analysis for homologous genes

Identification of homologous genes

Protein sequences were analyzed to identify homology across the three isolates by using the *Inparanoid* software [36] and a pair-wise analysis was also performed to identify the homology between any two strains by using the MultiParanoid software [37].

Differential gene expression

Based on the gene annotations in the database, the RPKM values were calculated for each gene using uniquely-mapped reads [38]. Raw read counts of genes were calculated by using HTSeq [39], BEDTools [35] and RSeQC [34]. Furthermore, DEGseq [40] was used to identify DEGs with the MARS model, with the criteria of fold change > 2 and $P < 0.05$.

Pathway analysis

Candidate genes were first mapped onto functional groups in COG; Gene Ontology and KEGG pathway analyses were performed online using the DAVID software [41] (Fisher's exact test, $P < 0.05$).

Virulence factor analysis

Virulence factors were extracted from the virulence factor database (VFDB) [42]. A VFs.faa file was used for local blasting with BLASTP (v2.2.24, using default parameter with E

value set as $1E-5$), and the top hits were used as candidates for further analysis.

Gene annotation of the *S. suis* 2 genome using RNA-seq data

Identification of novel TARs in intergenic regions

The sequencing depth for each nucleotide was first calculated, and a nucleotide was defined to be transcriptionally-active when its sequencing depth was higher than the lower deciles of the sequencing depth in the transcriptome. Consecutive transcriptionally-active nucleotides form TARs. In this study, TARs > 70 bp in intergenic regions were further annotated [43].

Annotation of novel genes

The DNA sequences for all novel TARs were blasted against NCBI Bacterial Genomes (all.ffn.tar.gz) for homology identification using BLAT. The functions of the novel TARs in three *S. suis* 2 isolates were annotated based on the function of their known homologous genes in other bacteria.

Identification of sRNAs

TARs without identified homologous genes were further compared with sRNAs in both sRNAMAP [44] using BLAT(V35) [45] and Rfam (11.0) using INFERNAL(1.1rc2) [46] to identify the potential sRNAs.

Authors' contributions

CZ conceived the project. DZ, ND and SM designed the experiments and performed the data analysis. SM and GL prepared all the samples. QH, GL and WC participated in sequencing experiments and data analysis. DZ, ND and CZ wrote the manuscript. All the authors read and approved the final manuscript.

Competing interests

The authors have declared no competing interests.

Acknowledgements

We thank Joel Haywood (Institute of Microbiology, Chinese Academy of Sciences, China) for proofreading and copyediting. This research was supported by the CAS Key Laboratory of Pathogenic Microbiology and Immunology of China (Grant No. 2009CASPMI-007) to DZ and the National Natural Science Foundation of China (Grant No. 81201700) to DZ.

Supplementary material

Supplementary material associated with this article can be found, in the online version, at <http://dx.doi.org/10.1016/j.gpb.2014.11.001>.

References

- [1] Wertheim HF, Nghia HD, Taylor W, Schultz C. *Streptococcus suis*: an emerging human pathogen. Clin Infect Dis 2009;48:617–25.
- [2] Palmieri C, Varaldo PE, Facinelli B. *Streptococcus suis*, an emerging drug-resistant animal and human pathogen. Front Microbiol 2011;2:235.
- [3] Tan JH, Yeh BI, Seet CS. Deafness due to haemorrhagic labyrinthitis and a review of relapses in *Streptococcus suis* meningitis. Singapore Med J 2010;51:e30–3.
- [4] Chen C, Tang J, Dong W, Wang C, Feng Y, Wang J, et al. A glimpse of streptococcal toxic shock syndrome from comparative genomics of *S. suis* 2 Chinese isolates. PLoS One 2007;2:e315.
- [5] Ma E, Chung PH, So T, Wong L, Choi KM, Cheung DT, et al. *Streptococcus suis* infection in Hong Kong: an emerging infectious disease? Epidemiol Infect 2008;136:1691–7.
- [6] Kerdsin A, Dejsirilert S, Puangpatra P, Sripakdee S, Chumla K, Boonkerd N, et al. Genotypic profile of *Streptococcus suis* serotype 2 and clinical features of infection in humans, Thailand. Emerg Infect Dis 2011;17:835–42.
- [7] Li W, Wan Y, Tao Z, Chen H, Zhou R. A novel fibronectin-binding protein of *Streptococcus suis* serotype 2 contributes to epithelial cell invasion and *in vivo* dissemination. Vet Microbiol 2013;162:186–94.
- [8] Feng Y, Zhang H, Ma Y, Gao GF. Uncovering newly emerging variants of *Streptococcus suis*, an important zoonotic agent. Trends Microbiol 2010;18:124–31.
- [9] Charland N, Harel J, Kobisch M, Lacasse S, Gottschalk M. *Streptococcus suis* serotype 2 mutants deficient in capsular expression. Microbiology 1998;144:325–32.
- [10] Xu J, Fu S, Liu M, Xu Q, Bei W, Chen H, et al. The two-component system NisK/NisR contributes to the virulence of *Streptococcus suis* serotype 2. Microbiol Res 2014;169:541–6.
- [11] Shen X, Zhong Q, Zhao Y, Yin S, Chen T, Hu F, et al. Proteome analysis of the two-component SalK/SalR system in Epidemic *Streptococcus suis* serotype 2. Curr Microbiol 2013;67:118–22.
- [12] Wang H, Shen X, Zhao Y, Wang M, Zhong Q, Chen T, et al. Identification and proteome analysis of the two-component VirR/VirS system in epidemic *Streptococcus suis* serotype 2. FEMS Microbiol Lett 2012;333:160–8.
- [13] Han H, Liu C, Wang Q, Xuan C, Zheng B, Tang J, et al. The two-component system Ihk/Irr contributes to the virulence of *Streptococcus suis* serotype 2 strain 05ZYH33 through alteration of the bacterial cell metabolism. Microbiology 2012;158:1852–66.
- [14] Li J, Tan C, Zhou Y, Fu S, Hu L, Hu J, et al. The two-component regulatory system CiaRH contributes to the virulence of *Streptococcus suis* 2. Vet Microbiol 2011;148:99–104.
- [15] Li M, Wang C, Feng Y, Pan X, Cheng G, Wang J, et al. SalK/SalR, a two-component signal transduction system, is essential for full virulence of highly invasive *Streptococcus suis* serotype 2. PLoS One 2008;3:e2080.
- [16] Jiang H, Fan HJ, Lu CP. Identification and distribution of putative virulent genes in strains of *Streptococcus suis* serotype 2. Vet Microbiol 2009;133:309–16.
- [17] Li M, Shen X, Yan J, Han H, Zheng B, Liu D, et al. GI-type T4SS-mediated horizontal transfer of the 89K pathogenicity island in epidemic *Streptococcus suis* serotype 2. Mol Microbiol 2011;79:1670–83.
- [18] Croucher NJ, Thomson NR. Studying bacterial transcriptomes using RNA-seq. Curr Opin Microbiol 2010;13:619–24.
- [19] Romilly C, Lays C, Tomasini A, Caldelari I, Benito Y, Hammann P, et al. A non-coding RNA promotes bacterial persistence and decreases virulence by regulating a regulator in *Staphylococcus aureus*. PLoS Pathog 2014;10:e1003979.

- [20] Wootton L. Bacterial pathogenesis: sRNA clears the way for G4. *Nat Rev Microbiol* 2013;11:146.
- [21] Lamichhane G, Arnvig KB, McDonough KA. Definition and annotation of (myco) bacterial non-coding RNA. *Tuberculosis* 2013;93:26–9.
- [22] Mellin JR, Cossart P. The non-coding RNA world of the bacterial pathogen *Listeria monocytogenes*. *RNA Biol* 2012;9:372–8.
- [23] Wurtzel O, Sapra R, Chen F, Zhu Y, Simmons BA, Sorek R. A single-base resolution map of an archaeal transcriptome. *Genome Res* 2010;20:133–41.
- [24] Passalacqua KD, Varadarajan A, Ondov BD, Okou DT, Zwick ME, Bergman NH. Structure and complexity of a bacterial transcriptome. *J Bacteriol* 2009;191:3203–11.
- [25] Sittka A, Lucchini S, Papenfort K, Sharma CM, Rolle K, Binnewies TT, et al. Deep sequencing analysis of small noncoding RNA and mRNA targets of the global post-transcriptional regulator, Hfq. *PLoS Genet* 2008;4:e1000163.
- [26] Lally ET, Hill RB, Kieba IR, Korostoff J. The interaction between RTX toxins and target cells. *Trends Microbiol* 1999;7:356–61.
- [27] Khoo SK, Loll B, Chan WT, Shoeman RL, Ngoo L, Yeo CC, et al. Molecular and structural characterization of the PezAT chromosomal toxin–antitoxin system of the human pathogen *Streptococcus pneumoniae*. *J Biol Chem* 2007;282:19606–18.
- [28] Boyle MD, Raeder R, Flosdorff A, Podbielski A. Role of *emm* and *mvp* genes in the virulence of group A streptococcal isolate 64/14 in a mouse model of skin infection. *J Infect Dis* 1998;177:991–7.
- [29] Gorke B, Stulke J. Carbon catabolite repression in bacteria: many ways to make the most out of nutrients. *Nat Rev Microbiol* 2008;6:613–24.
- [30] Deutscher J, Francke C, Postma PW. How phosphotransferase system-related protein phosphorylation regulates carbohydrate metabolism in bacteria. *Microbiol Mol Biol Rev* 2006;70:939–1031.
- [31] Vu-Khac H, Miller KW. Regulation of mannose phosphotransferase system permease and virulence gene expression in *Listeria monocytogenes* by the EII(t)Man transporter. *Appl Environ Microbiol* 2009;75:6671–8.
- [32] Rothe FM, Bahr T, Stulke J, Rak B, Gorke B. Activation of *Escherichia coli* antiterminator BglG requires its phosphorylation. *Proc Natl Acad Sci U S A* 2012;109:15906–11.
- [33] Beloin C, Michaelis K, Lindner K, Landini P, Hacker J, Ghigo JM, et al. The transcriptional antiterminator RfaH represses biofilm formation in *Escherichia coli*. *J Bacteriol* 2006;188:1316–31.
- [34] Wang L, Wang S, Li W. RSeQC: quality control of RNA-seq experiments. *Bioinformatics* 2012;28:2184–5.
- [35] Quinlan AR, Hall IM. BEDTools: a flexible suite of utilities for comparing genomic features. *Bioinformatics* 2010;26:841–2.
- [36] O'Brien KP, Remm M, Sonnhammer EL. Inparanoid: a comprehensive database of eukaryotic orthologs. *Nucleic Acids Res* 2005;33:D476–80.
- [37] Alexeyenko A, Tamas I, Liu G, Sonnhammer EL. Automatic clustering of orthologs and inparalogs shared by multiple proteomes. *Bioinformatics* 2006;22:e9–15.
- [38] Mortazavi A, Williams BA, McCue K, Schaeffer L, Wold B. Mapping and quantifying mammalian transcriptomes by RNA-Seq. *Nat Methods* 2008;5:621–8.
- [39] Anders S, Pyl PT, Huber W. HTSeq — a python framework to work with high-throughput sequencing data. *Bioinformatics* 2014. <http://dx.doi.org/10.1093/bioinformatics/btu638>.
- [40] Wang L, Feng Z, Wang X, Wang X, Zhang X. DEGseq: an R package for identifying differentially expressed genes from RNA-seq data. *Bioinformatics* 2010;26:136–8.
- [41] Huang DW, Sherman BT, Lempicki RA. Systematic and integrative analysis of large gene lists using DAVID bioinformatics resources. *Nat Protoc* 2008;4:44–57.
- [42] Chen L, Xiong Z, Sun L, Yang J, Jin Q. VFDB 2012 update: toward the genetic diversity and molecular evolution of bacterial virulence factors. *Nucleic Acids Res* 2012;40:D641–5.
- [43] Reddy JS, Kumar R, Watt JM, Lawrence ML, Burgess SC, Nanduri B. Transcriptome profile of a bovine respiratory disease pathogen: *Mannheimia haemolytica* PHL213. *BMC Bioinformatics* 2012;13:S4.
- [44] Huang HY, Chang HY, Chou CH, Tseng CP, Ho SY, Yang CD, et al. sRNAMap: genomic maps for small non-coding RNAs, their regulators and their targets in microbial genomes. *Nucleic Acids Res* 2009;37:D150–4.
- [45] Kent WJ. BLAT — the BLAST-like alignment tool. *Genome Res* 2002;12:656–64.
- [46] Burge SW, Daub J, Eberhardt R, Tate J, Barquist L, Nawrocki EP, et al. Rfam 11.0: 10 years of RNA families. *Nucleic Acids Res* 2013;41:D226–32.